

Effects of co-plasticization of acetyl tributyl citrate and glycerol on the properties of starch/PVA films

Wentao Wang, Enjie Diao, Hui Zhang, Yangyong Dai, Hanxue Hou, Haizhou Dong

School of Food Science and Engineering, Shandong Agricultural University, Tai'an 271018, P.R. China

Correspondence to: H. Hou (E-mail: hhx@sdau.edu.cn) and H. Dong (E-mail: hzhdong28@126.com)

ABSTRACT: Starch/polyvinyl alcohol (PVA) nanocomposite films by film blowing process were successfully obtained. Starch (1700 g), PVA (300 g), and organically modified montmorillonite (OMMT, 200 g) were blended and plasticized with acetyl tributyl citrate (ATBC) and glycerol (GLY) at weight ratios of 0/100, 5/95, 10/90, 15/85, 20/80, and 25/75. The structural, morphology, barrier, mechanical, and thermal properties of the films, as well as molecular interactions in the nanocomposites were analyzed. The 3.98 nm *d*-spacing was the highest in starch/PVA nanocomposite films plasticized with ATBC/GLY ratio of 10/90. The film with ATBC/GLY (5/95) had the lowest WVP ($3.01 \times 10^{-10} \text{ g m}^{-1} \text{ s}^{-1} \text{ Pa}^{-1}$). The longitudinal tensile strength (TS) of starch/PVA nanocomposite films gradually increased from 4.46 to 6.81 MPa with the increase of ATBC/GLY ratios. The T_g steadily increased from 49.2°C to 55.2°C and the ΔH of the nanocomposite films decreased from 81.77 to 51.43 J/g at the presence of ATBC. The addition of ATBC into GLY plasticized starch/PVA/OMMT system enhanced the intermolecular interaction in the nanocomposites. This study proved that ATBC was an excellent compatibilizer in the preparation of starch/PVA/OMMT nanocomposite films. © 2015 Wiley Periodicals, Inc. *J. Appl. Polym. Sci.* **2015**, *132*, 42544.

KEYWORDS: biodegradable; clay; extrusion; films; hydrophilic polymers

Received 25 February 2015; accepted 26 May 2015

DOI: 10.1002/app.42544

INTRODUCTION

The increased nonbiodegradable plastic wastes has become a major source of pollution, which has been a worldwide environmental problem, therefore, biodegradable polymers for packaging materials have attracted much attention in recent years.¹ Starch-based film is one of the most promising biodegradable polymers because of its good gas barrier properties, transparency, biodegradability, cost efficiency, and availability.^{2,3} Polyvinyl alcohol (PVA) is a colorless, nontoxic, and widely available biodegradable polymer with excellent film-forming capabilities.⁴ The PVA films exhibit great tensile strength and flexibility as well as enhanced oxygen and aroma barrier properties.⁵ Starch and PVA blends are widely studied among biodegradable materials.

However, the mechanical properties and moisture barrier properties of starch/PVA blends should be further improved in some practical fields. The performances of starch/PVA blends have been enhanced by acid modification and plasma treatment,⁶ addition of cross-linking agents⁷ and blending plasticizers,⁸ or addition of nanoparticles.^{9–11} Starch/PVA nanocomposites have great advantages because of their enhanced mechanical properties and moisture barrier properties. Majdzadeh-Ardakani *et al.*¹² reported that starch/PVA/clay nanocomposites with

organically modified montmorillonite (OMMT) exhibited better mechanical properties than those of unmodified montmorillonite (MMT). Gao *et al.*¹³ reported that natural and organically modified clays tended to form nanocomposites with native and modified starches, respectively. In the perfect nanocomposites, the clay platelets uniformly dispersed in the polymer matrix with intercalated or exfoliated structures other than the aggregation as tactoids.¹⁴ However, compared to starch nanocomposites and PVA nanocomposites, starch/PVA nanocomposite have not been widely studied.

Starch/PVA composites were prepared with various plasticizers.¹⁰ Glycerol (GLY) and water have been used as plasticizers for starch/PVA blends.^{15,16} Some commonly used plasticizers include sorbitol,^{17,18} urea,¹⁹ citric acid,^{17,20} and GLY–urea mixture.⁸ However, all these plasticizers are hydrophilic compounds which generally lead to high water vapor permeability and poor dispersion of OMMT in the starch/PVA matrix.

Acetyl tributyl citrate (ATBC) is an eco-friendly, hydrophobic plasticizer that has been applied for biomedical and biodegradable materials.²¹ This plasticizer has been used in some polymers, such as PVC,²² PLA,^{21,23,24} PHA,²⁵ and PHB²⁶ to maintain the softness and pliability of the plastics and rubbers. The hydrophobic ATBC and hydrophilic GLY can be combined

to yield a mixed plasticizer that can improve the performances of starch/PVA nanocomposite films.

Starch/PVA films have been primarily prepared by solution casting since the 1980s. However, large-scale production of starch/PVA films by solution process has not been encouraged because it involves higher processing costs and lower production efficiency compared with extrusion process.¹⁰ Extrusion blowing can be applied in industrial production of starch/PVA film because of its high productivity and efficiency. Nevertheless, there have been very few studies on starch/PVA film by extrusion blowing process.

In this study, extrusion blowing was performed to prepare starch/PVA nanocomposite films which were co-plasticized by ATBC and GLY. The influences of different ATBC/GLY ratios on the formation of nanostructure and properties of starch/PVA films were investigated first.

EXPERIMENTAL

Materials

Hydroxypropyl distarch phosphate (mode HP-CF T0278, HPDSP) was purchased from Puluoxing Starch (Hangzhou, China). The moisture and hydroxypropyl group content of the HPDSP were 13.2% and 3.1%, respectively. Poly(vinyl alcohol) (PVA) was obtained from Sinopec Sichuan Vinylon Works (Chongqing, China), with polymerization degree of 1700, alcoholysis degree of 99.0%, and ash of less than 0.6%. GLY was purchased from Chemical Reagent (Tianjin, China). ATBC was obtained from Jiangsu Lemon Chemical and Technology (Jiangsu, China). Organically modified montmorillonite (OMMT) with octadecyl benzyl ammonium as cation was obtained from Zhejiang Fenghong (Zhejiang, China).

Blending and Compounding

HPDSP (1700 g), PVA (300 g), and OMMT (200 g) were thoroughly blended in a SHR50A mixer (Hongji, Zhangjiagang, China) at room temperature for 10 min. ATBC was mixed with GLY at weight ratios of 0/100, 5/95, 10/90, 15/85, 20/80, and 25/75 with a high speed blender (Ultraturrax T18, IKA, Stauffen, Germany) for 5 min at 10,000 rpm. The mixed plasticizers (700 g) were slowly added into the starch/PVA/OMMT blends and mixed for 15 min at room temperature. The mixtures were then packaged in polyethylene bags and stored for 24 h at room temperature to equilibrate all the components. The mixtures were then compounded in a laboratory twin screw extruder (Jingrui Plastic Machinery, Laiwu, China) with a screw diameter of 35 mm, screw length of 30D, and two individually controlled temperature zones. Compounding was performed at a screw speed of 50 rpm and at 80°C and 120°C in barrel zones I and II, respectively. The extruded strands were cut into pellets and conditioned for at least 72 h at 23 ± 2°C and 53% relative humidity (RH) prior to film blowing.

Film Blowing

The starch/PVA nanocomposite films were prepared by extrusion blowing using a single screw extruder (Jingrui Plastic Machinery, Laiwu, China) with a screw diameter of 35 mm, screw length of 25D, screw compression ratio of 3 : 1 and four individually controlled temperature zones. The extruder was equipped with a con-



Figure 1. Continuous and stable preparation of starch/PVA nanocomposite films. [Color figure can be viewed in the online issue, which is available at wileyonlinelibrary.com.]

ventional temperature-controlled film-blowing die with a diameter of 60 mm and a film-blowing tower with a calendaring nip and takeoff rolls. Temperatures in the barrel and die were set at 80°C, 130°C, 140°C, 150°C, and 145°C from feed inlet to die, respectively. The ratio of the diameter of the die to that of the blown bubble (BUR) was carefully set at 1 : 4. The ratio of the take-up velocity to the film velocity at the die exit (TUR) was carefully set at 4 : 3. Figure 1 showed the continuous and stable preparation of starch/PVA nanocomposite films.

Structural Characterization

X-ray diffraction (XRD) was performed with a D8 Advance X-ray diffractometer (Bruker-AXS, Germany). Film samples were previously conditioned in a desiccator at 23 ± 2°C and 53% RH prior to determination. The samples were then scanned at diffraction angles (2θ) from 1° to 40° at a speed of 0.02°/s. Transmission electron microscopy (TEM) was performed with a Tecnai 20U-TWIN electron microscope (Philips, the Netherlands) at an operating voltage of 100 kV. Ultra-fine grinding samples were placed onto a carbon-coated copper grid by physical grid-powder interactions. The dispersion of the clays was investigated.

Film Properties

Water vapor permeability (WVP) was measured according to the ASTM E96-95 with modifications using an automatic water vapor permeability tester (PERMETM W3/030, Jinan, China). Films were cut into round shape (80 mm in diameter) with a special sampler. The specimens were placed in the environment of 23 ± 2 and 50 ± 5% RH for at least 72 h prior to testing. The test was carried out at 38°C and 90% RH. The WVP of each sample was obtained from the average of three measurements.

Tensile strength (TS, MPa) and elongation at break (E , %) of the films were measured with a TA-XT2i texture analyzer (Stable Micro System, UK) at 23 ± 2°C and 53% RH according to ASTM D882-02. The samples were cut into strips (dimensions, 120 mm × 15 mm) in the horizontal and longitudinal directions of the extruder with a sharp knife and conditioned at 23 ± 2°C and 53% RH for 7 days prior to the measurements. The initial distance between the grips was 50 mm. The cross-head speed was set at 1 mm/s. Each test was composed of six

replicate measurements. TS and E were calculated according to previous study.¹⁴

Differential Scanning Calorimetry

The glass transition temperatures (T_g), melting temperature (T_m), and melting enthalpy (ΔH) of the samples were determined with a DSC 200PC (NETZSCH Scientific Instruments, Germany) with a thermal analysis software (version 4.8) at a heating rate of 10°C/min from -50°C to 250°C. All the film samples were conditioned for 72 h at $23 \pm 2^\circ\text{C}$ and 53% RH prior to the measurement. Each test was composed of three replicate measurements. Glass transition temperatures were determined from resulting thermograms as the midpoint between onset and end temperatures of step changes in heat flow observed during heating.

Fourier-Transform Infrared Spectroscopy

The fourier-transform infrared (FTIR) spectra of the films were obtained using a Thermo Fisher Scientific (USA) Nexus 670 spectrometer attached to a Smart iTR diamond ATR accessory for wavelengths ranging from 3700 to 900 cm^{-1} . The number of accumulated scans and the scanning rate were 32 and 4 cm^{-1} , respectively. The film was directly mounted in the sample holder and tested.²⁷

Statistical Analysis

Statistical differences of the properties of different samples were analyzed with ANOVA via SPSS (version 17.0, SPSS, Chicago, USA). Duncan's multiple range test was performed to compare the mean values of film properties when $P < 0.05$.

RESULTS AND DISCUSSION

Structural Characteristics of Starch/PVA Nanocomposite Films

XRD provides information on the intercalated and exfoliated nanostructures in polymer/clay nanocomposites. During intercalation, polymer molecules enter the OMMT galleries and increase the gallery spacing.²⁸ Bragg's law states that the increase in d -spacing results in a shift of the diffraction peak towards low angles. Figure 2 showed the effects of the ATBC/GLY weight ratios on the XRD patterns of starch/PVA nanocomposite films. The nanocomposite films plasticized with ATBC/GLY exhibited peaks at low angles in contrast to OMMT (Figure 2). A characteristic peak at $2\theta = 2.900^\circ$ (d -spacing, 3.06 nm) was observed for OMMT. The starch/PVA nanocomposite film plasticized by pure GLY exhibited a peak at $2\theta = 2.382^\circ$ (d -spacing, 3.68 nm). In contrast, the films prepared with mixed plasticizers (ATBC/GLY = 5/95, 10/90, 15/85, 20/80, and 25/75) showed peaks at $2\theta = 2.313^\circ$, 2.244° , 2.313° , 2.278° , and 2.313° corresponding to d -spacing of 3.87, 3.98, 3.87, 3.94, and 3.87 nm, respectively. The increased d -spacing indicated the formation of co-intercalated structures because of the starch and/or PVA molecule chains in the OMMT galleries. The films with the mixed plasticizers exhibited higher d -spacing than that plasticized with pure GLY (ATBC/GLY = 0/100), suggesting that the starch/PVA blends strongly interacted with OMMT at the presence of ATBC. The d -spacing was the highest for the films plasticized with ATBC/GLY (10/90). Starch and/or PVA molecules sufficiently entered the OMMT galleries with dominant peaks that

shifted from 2.900° (d -spacing, 3.06 nm) to 2.244° (d -spacing, 3.98 nm). These results indicated that ATBC/GLY (10/90) facilitated the formation of intercalated nanocomposites between starch/PVA and OMMT.

The intercalated structures in starch/PVA nanocomposites were confirmed by the TEM images. Tang *et al.*¹⁴ reported that TEM qualitatively elucidated the internal structure, spatial distribution, and dispersion of nanoparticles in the polymer matrix through direct visualization. Figure 3 shows the TEM images of starch/PVA nanocomposite films for different ATBC/GLY ratios. The nanocomposite films plasticized with ATBC/GLY (5/95, 10/90) exhibited obvious multilayer nanostructures [Figure 3(b,c)]. The film plasticized with pure GLY (ATBC/GLY = 0/100) showed very few intercalation of starch/PVA molecules into clay galleries, but exhibited particle agglomerates or tactoids [dark spots in Figure 3(a)]. These results were in agreement with the XRD patterns. ATBC as a secondary plasticizer added to the starch/PVA composite played a compatibilizer role in this study. The hydrophilicity of the starch/PVA matrix was reduced and became similar to that of OMMT at the ATBC/GLY ratio of 10/90. Hence, the dispersion and intercalation of OMMT in the starch matrix were improved. The hydrophilicity of the starch/PVA matrix with higher ATBC/GLY ratios (25/75) was relatively poor compared to that of OMMT which hindered the formation of intercalated nanostructures.

Zeppa *et al.*²⁹ reported that hydrophilic MMT- Na^+ dispersed well in starch matrix plasticized by either glycerol or urea/ethanolamine mixture (50/50) while organically modified montmorillonite (Cloisite 30B) agglomerated and could hardly form a nanocomposite with starch. The authors attributed the results to the polar structure of the plasticizers used in their study. Hydrophobic plasticizers should receive more attention in improving the dispersion of OMMT in polar polymer matrix.

Water Vapor Barrier Property of Starch/PVA Nanocomposite Films

The water vapor permeability of starch/PVA films was one of the most important properties of starch/PVA films when used in packaging. Figure 4 illustrated the water vapor barrier properties of the starch/PVA nanocomposite films. The film without ATBC exhibited the highest water vapor permeability ($6.16 \times 10^{-10} \text{ g m}^{-1} \text{ s}^{-1} \text{ Pa}^{-1}$), while the film with ATBC/GLY (5/95) had the lowest WVP ($3.01 \times 10^{-10} \text{ g m}^{-1} \text{ s}^{-1} \text{ Pa}^{-1}$). These results indicated that the addition of ATBC in starch/PVA matrix improved the water vapor barrier properties of the films. The transmission of water vapor through hydrophilic films depended on the diffusivity and solubility of water molecules in the film matrix. When the nanocomposite was formed, the impermeable clay platelets created a tortuous pathway for the water molecules to traverse the film matrix, thereby increasing the effective path length for diffusion.¹⁴ The WVP of the starch/PVA nanocomposite films plasticized with ATBC/GLY mixture was reduced because of the perfect formation of intercalated nanostructures. Pure GLY yielded less intercalated structure in the starch/PVA matrix and the corresponding sample exhibited poor water vapor barrier property.³⁰

Figure 4 showed that WVPs slightly increased and then decreased with the increase of ATBC/GLY ratios (5/95, 10/90,

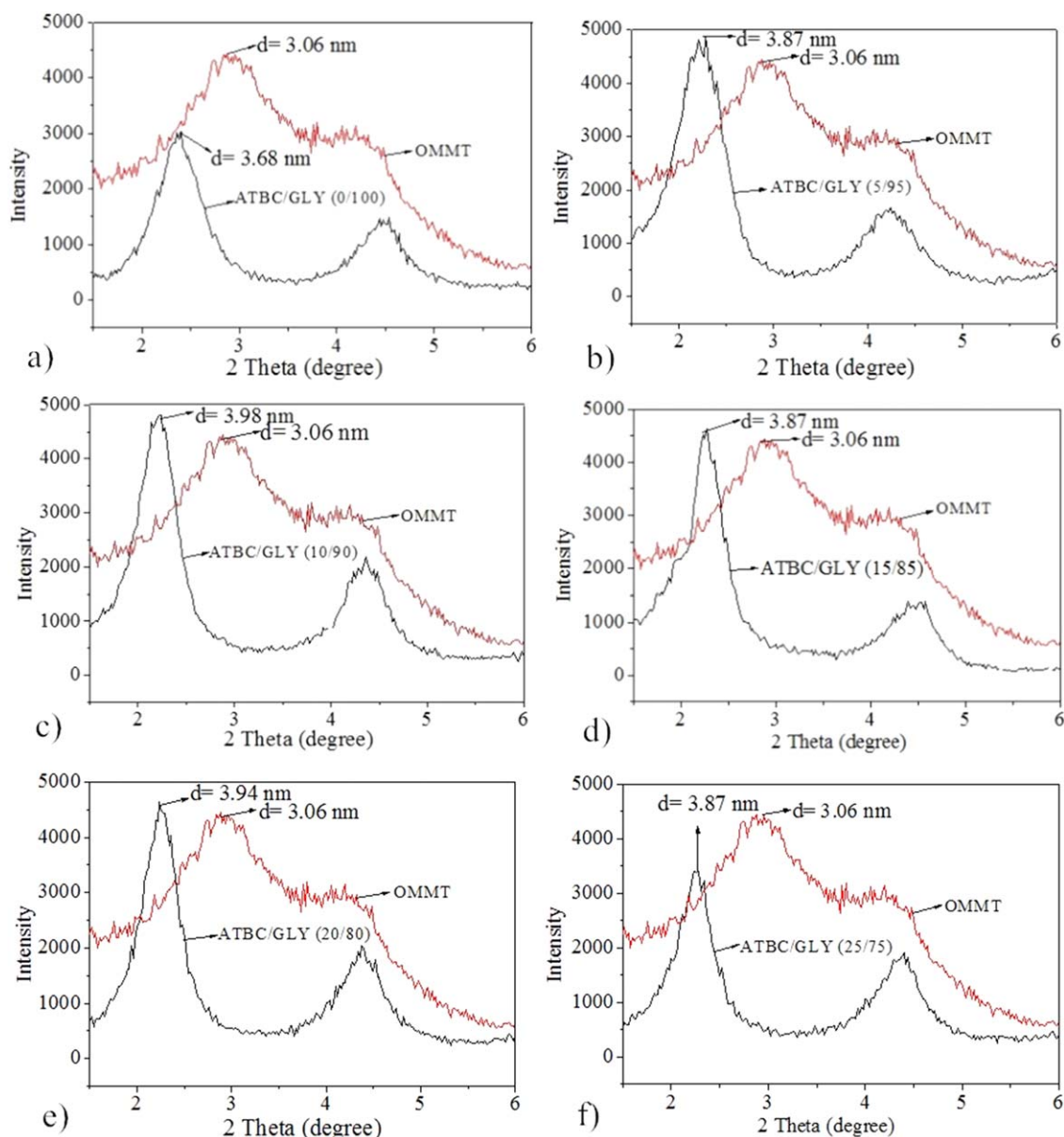


Figure 2. XRD patterns of OMMT and starch/PVA nanocomposite films with different weight ratios of ATBC and GLY: (a) 0/100, (b) 5/95, (c) 10/90, (d) 15/85, (e) 20/80, and (f) 25/75. [Color figure can be viewed in the online issue, which is available at wileyonlinelibrary.com.]

15/85, 20/80, and 25/75). The WVP of the film was also influenced by the hydrophilic property and the homogeneity of the polymer matrix.³¹ ATBC could reduce the WVP of the nanocomposite films partly because it is hydrophobic. The hydrophilicity of the mixed ATBC/GLY (5/95) plasticizer was exactly similar to that of the starch/PVA/OMMT system. The film components could homogeneously disperse in the polymer matrix, thereby reducing the WVP. More hydrophobic ATBC insignificantly improved the water vapor barrier properties of the films because of the poor homogeneity of the film-forming components (shown in TEM images).

Mechanical Properties of Starch/PVA Nanocomposite Films

The mechanical properties of starch/PVA nanocomposite films were determined in longitudinal and horizontal directions,

which were parallel and perpendicular to the die (Figure 1), respectively. Figure 5 showed the TS and *E* of the nanocomposite films based on various ATBC/GLY ratios.

The longitudinal TS of starch/PVA nanocomposite films gradually increased from 4.46 to 6.81 MPa with the increase of ATBC/GLY ratios [Figure 5(a)]. The starch/PVA nanocomposite films with ATBC/GLY ratios of 15/85 and 20/80 had the highest TS. This may be because of the higher interfacial and/or intermolecular interaction in the starch/PVA matrix.³² Sreekumar *et al.*³³ reported that starch/PVA blend at the ratio of 30/70 was the most compatible blend and the compatibility decreased with the increase in starch content. In this study, the ratio of starch/PVA was much higher than 30/70. As mentioned above, addition of ATBC improved compatibilities between starch, PVA

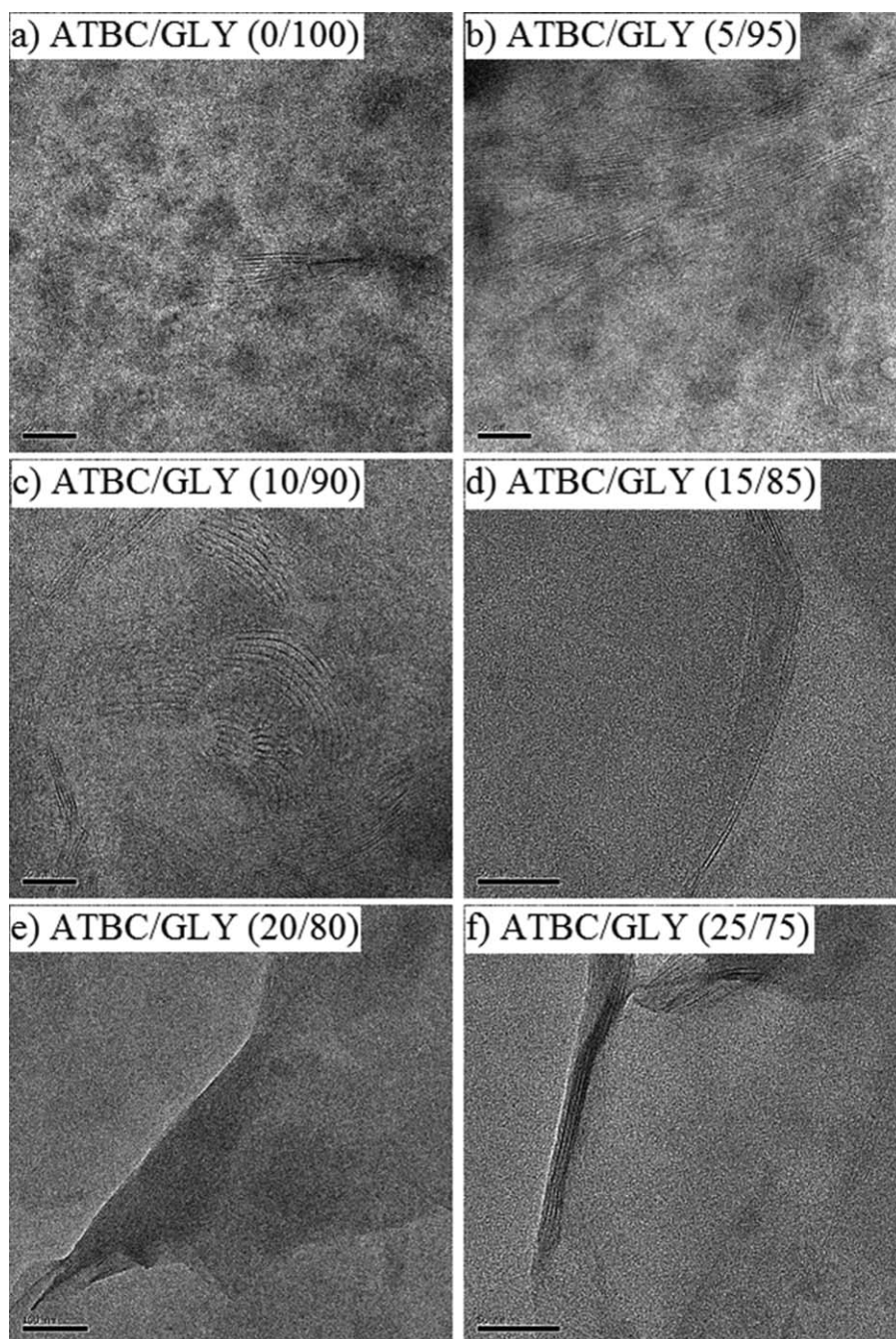


Figure 3. TEM micrographs of starch/PVA nanocomposite films with different weight ratios of ATBC and GLY: (a) 0/100, (b) 5/95, (c) 10/90, (d) 15/85, (e) 20/80, and (f) 25/75.

and OMMT. At lower and higher ATBC/GLY ratios, the decrease of TS may be ascribed to agglomeration of OMMT. Lai *et al.*³⁴ reported that some hydrophobic plasticizers (e.g., palmitic and stearic acids) beneficially strengthened the zein films because of the strong polymer–plasticizer interactions. On the other hand, the intercalated nanostructure in starch/PVA/OMMT composites with median ATBC/GLY ratios also contributed to higher TS.¹³

Figure 5(b) indicated that E of the films decreased with increase of ATBC/GLY ratios (5/95, 10/90, 15/85, 20/80, and 25/75). The

result suggested that the increased incorporation of ATBC decreased the motilities of starch and/or PVA molecules. Plasticizers were substances incorporated into a polymer to increase its flexibility, processability, and distensibility. These substances provided spacing for the polymer chains, which allowed the plastics to be soft, comfortable, and highly flexible. The addition of ATBC to starch/PVA blend showed an anti-plasticization effect. Similar results were obtained for other hydrophobic plasticizers.³⁵ The enhanced interactions between starch, PVA and OMMT prevented the facile sliding of the polymer chains and

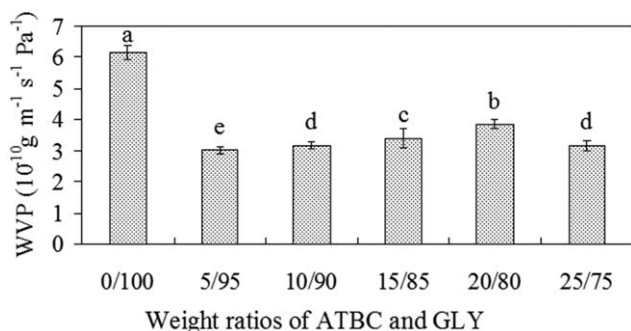


Figure 4. Water vapor permeabilities of starch/PVA nanocomposite films with different weight ratios of ATBC and GLY (0/100, 5/95, 10/90, 15/85, 20/80, 25/75).

thereby lowered the elongation properties of the nanocomposites.³⁶

The longitudinal and horizontal mechanical properties of starch/PVA nanocomposite films were also compared in Figure 5. The TS in the longitudinal direction was higher than that in the horizontal direction. This result was in agreement with that of a previous study³⁷ which reported that the TS of hydroxypropylated and oxidized potato starch films were higher in the longitudinal direction than those in the horizontal direction.

Thermal Transition of Starch/PVA Nanocomposite Films

Differential scanning calorimetry (DSC) has proven to be a very effective analytical tool to characterize the glass transition (T_g), melting temperature (T_m), and the corresponding enthalpy changes of polymers and polymer composites. The data from DSC can be used to elucidate the compatibilities and existing states of various components in composites.³⁶ The DSC curves

of the films exhibited single melting endotherms in Figure 6 which indicated that the components of the films were compatible on the whole.³⁸ The DSC curves of the films became more and more smooth with the increase of the ATBC/GLY ratios which illustrated that addition of ATBC improved the compatibility of the components in the films. The T_g , T_m , and melting enthalpy (ΔH) of starch/PVA/OMMT nanocomposites with different ATBC/GLY ratios were showed in Table I. The T_g of the nanocomposite films were 49.2°C, 50.5°C, 51.3°C, 51.9°C, 54.4°C, and 55.2°C for the ATBC/GLY ratios of 0/100, 5/95, 10/90, 15/85, 20/80, 25/75, respectively. The T_g steadily increased with increasing ATBC/GLY ratios, which indicated that the molecular interactions were enhanced and molecular mobility was inhibited in the nanocomposites at the presence of ATBC.³⁹ This may be attributed to the improved dispersion of OMMT and the additional formation of intercalated nanostructure.⁴⁰ Ali *et al.*³⁶ reported similar effects of OMMT on the polymer relaxation behavior and the T_g of the nanocomposites which depended on the interplay between the confinement of polymer chains, surface interactions, and the formation of intermolecular structures.

The T_m of starch/PVA nanocomposite films with median ATBC/GLY ratios (10/90 and 15/85) was lower than that of the other nanocomposite films. This was probably related to the various crystal sizes and perfection in the films at the presence of heterogeneous nucleation of OMMT platelets.⁴¹ The ΔH of the nanocomposite films decreased from 81.77 to 51.43 J/g with the increase of ATBC/GLY ratios from 0/100 to 25/75. This may be because of either well-dispersed OMMT platelets or hydrophobic ATBC which hindered the starch and/or PVA chains mobility and then inhibited crystal growth and lowered the degree of crystallinity. On the other hand, the enhanced interactions between starch/PVA molecules and OMMT at the presence of ATBC also decreased the crystallinity and thus ΔH .⁴²

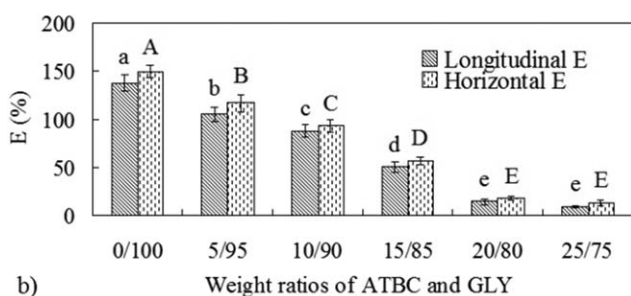
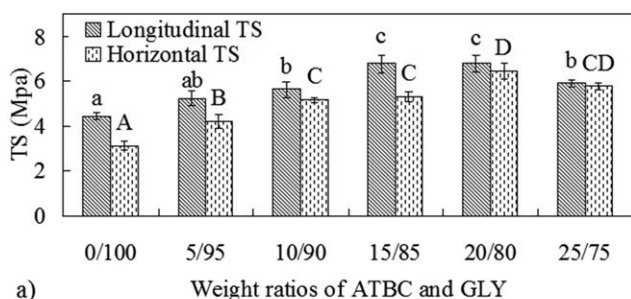


Figure 5. (a) Tensile strength and (b) elongation at break of starch/PVA nanocomposite films with different weight ratios of ATBC and GLY (0/100, 5/95, 10/90, 15/85, 20/80, 25/75).

Molecular Interactions of Starch/PVA Nanocomposite Films

The molecular interactions between polymers, plasticizers and OMMT were identified by FTIR spectral analysis. Given the spectral changes (e.g. peak shifting and broadening) of the composites with respect to the addition of each component, distinct chemical interactions (e.g., hydrogen bonds and dipolar interactions) were observed in the components.⁴³ The harmonic oscillator model states that the peak frequency decreases with increasing molecular interactions.⁴⁴

Figure 7 indicated the FTIR spectra of the starch/PVA nanocomposite films with different ATBC/GLY ratios. The typical peak at around 3340 cm^{-1} was the O-H stretching peak. The peak ascribed to the hydroxyl groups that participated in the formation of hydrogen bonds.⁴⁵ As shown in Figure 7(a), the peaks gradually shifted to lower wavenumbers (from 3341.7 to 3336.4 cm^{-1}) with the increase of ATBC/GLY ratios. The results indicated that new hydrogen bonds between starch and PVA chains formed at the presence of ATBC in the composites.¹² This may be because of the compatibilizing effect of ATBC which facilitated more interactions between starch and PVA molecules. The peak at around 2920 cm^{-1} was the methylene C-H stretch in glucose ring. In comparison to the film without

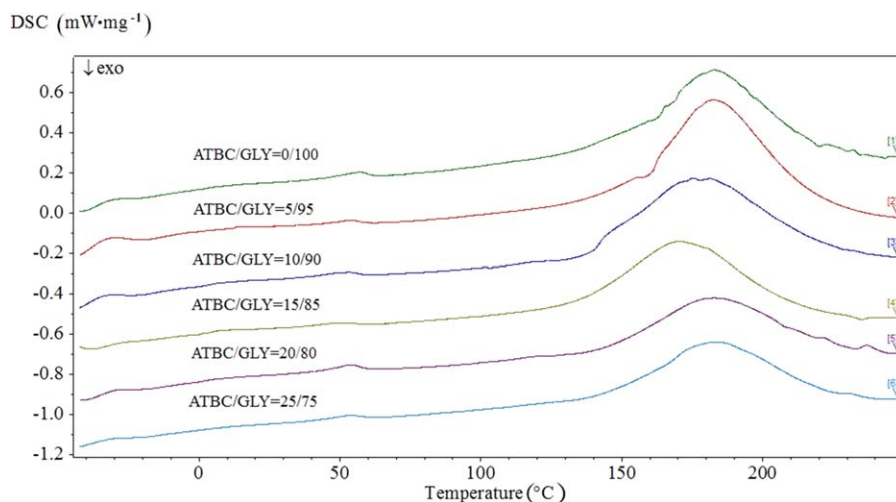


Figure 6. DSC curves of starch/PVA nanocomposite films with various ATBC/GLY ratios. [Color figure can be viewed in the online issue, which is available at wileyonlinelibrary.com.]

ATBC, the peaks gradually shifted to lower wavenumbers (from 2927.2 to 2920.4 cm^{-1}) with the increase of ATBC/GLY ratios. This implied that C-H ($-\text{CH}_2-$) bonds had also taken part in the formation of hydrogen bonds at the presence of ATBC.⁴⁶

Three characteristic peaks were observed between 1000 and 1200 cm^{-1} , which were attributed to C-O bond stretching of starch [Figure 7(b)]. The peak around 1150 cm^{-1} was ascribed to C-O bond stretching of the C-O-H group in starch, while the other two peaks around 1080 and 1040 cm^{-1} were attributed to C-O bond stretching of the C-O-C group in the anhydroglucose ring.⁴⁷ The strength of polymer-plasticizer interaction increased with decreasing peak frequency of the C-O group.⁴⁸ The peaks of C-O bond stretching at 1045.3, 1086.2, and 1156.3 cm^{-1} of the films without ATBC were shifted to 1030.0, 1080.9, and 1151.3 cm^{-1} for the films with ATBC/GLY ratio of 25/75, respectively. The O=C group of ATBC and -OH group of GLY formed hydrogen bonds with starch/PVA molecules, respectively. These peak shifts were related to the stability and intensity of hydrogen bonds that were formed between ATBC/GLY and C-O group of starch/PVA. Wang *et al.*⁴⁷ reported that citric acid as a second plasticizer increased the dispersion of montmorillonite and intermolecular interaction detected by FT-IR spectroscopy in the nanocomposite system.

Table I. Thermal Transition of Starch/PVA Nanocomposite Films with Different Weight Ratios of ATBC and GLY

Weight ratios of ATBC and GLY	T_g ($^{\circ}\text{C}$)	T_m ($^{\circ}\text{C}$)	ΔH_m (J/ g)
0/100	49.2	182.9	81.77
5/95	50.5	182.7	79.46
10/90	51.3	175.6	73.79
15/85	51.9	170.6	70.36
20/80	54.4	182.3	52.58
25/75	55.2	184.9	51.43

CONCLUSIONS

The ATBC/GLY ratios significantly influenced the formation of nanostructures, the water vapor barrier, mechanical and thermal

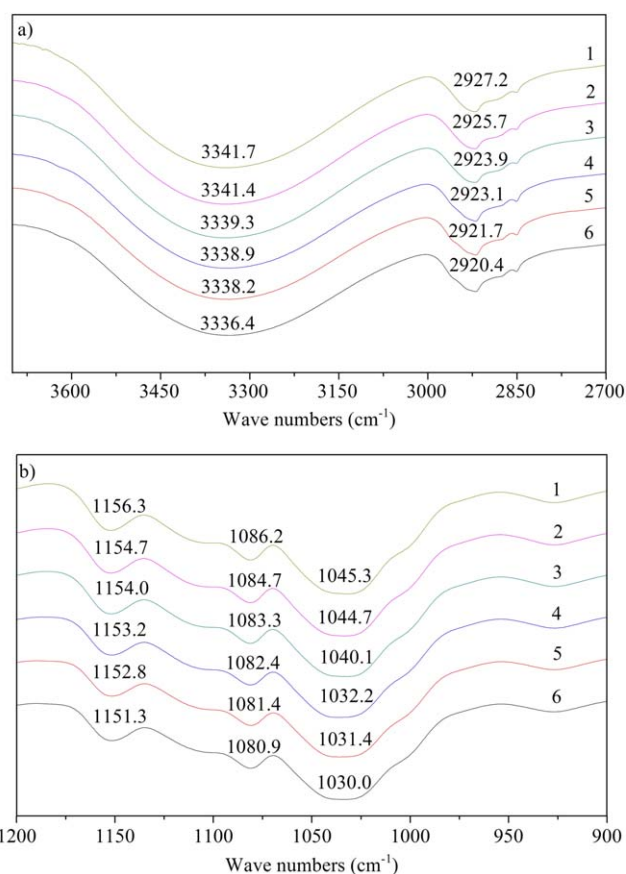


Figure 7. FTIR spectra of starch/PVA nanocomposite films with different weight ratios of ATBC and GLY (1-0/100, 2- /95, 3-10/90, 4-15/85, 5-20/80, 6-25/75). [Color figure can be viewed in the online issue, which is available at wileyonlinelibrary.com.]

properties as well as the molecular interactions of starch/PVA nanocomposite films prepared by extrusion blowing process. The ATBC/GLY ratio of 10/90 facilitated the perfect formation of intercalated nanocomposites between starch/PVA and OMMT. The films with ATBC/GLY of 5/95 exhibited improved moisture barrier properties (lowest WVP, $3.01 \times 10^{-10} \text{ g m}^{-1} \text{ s}^{-1} \text{ Pa}^{-1}$). The TS of the nanocomposite films increased with increasing ATBC/GLY ratios up to 20/80. Addition of ATBC increased T_g and decreased ΔH of the nanocomposite films. The mixed plasticizers (ATBC and GLY) produced highly stable and stronger hydrogen bonds in the starch/PVA/OMMT system. Hydrophobic plasticizers should be further studied to improve the dispersion of OMMT and performance of starch-based nanocomposites.

ACKNOWLEDGMENTS

The authors appreciate the financial support of the National Natural Science Foundation of China (31371747), the National Key Technology Support Program (2013BAD18B10-3) and the Natural Science Foundation of Shandong Province (ZR2012CM016). There is no any conflict of interest. The contribution of the authors: Wentao Wang: Preparation of starch/PVA nanocomposite films by extrusion blowing, analysis of XRD results and drafting the paper, Enjie Diao: Measurement and analysis of mechanical properties of the samples, Hui Zhang: Analysis of thermal properties of samples, Yangyong Dai: Measurement and analysis of water vapor permeabilities of the films, Hanxue Hou: Experimental design, FTIR and TEM analysis of the samples, and Haizhou Dong: Improvement of experimental design and revising the draft critically.

REFERENCES

1. Cano, A.; Fortunati, E.; Chafer, M.; Kenny, J. M.; Chiralt, A.; Gonzalez-Martinez, C. *Food Hydrocoll.* **2015**, *48*, 84.
2. Bonilla, J.; Talón, E.; Atarés, L.; Vargas, M.; Chiralt, A. *J. Food Eng.* **2013**, *118*, 271.
3. Menzel, C.; Olsson, E.; Plivelic, T. S.; Andersson, R.; Johansson, C.; Kuktaite, R.; Järnström, L.; Koch, K. *Carbohydr. Polym.* **2013**, *96*, 270.
4. Wang, S. Y.; Ren, J. L.; Li, W. Y.; Sun, R. C.; Liu, S. J. *Carbohydr. Polym.* **2014**, *103*, 94.
5. Priya, B.; Gupta, V. K.; Pathania, D.; Singha, A. S. *Carbohydr. Polym.* **2014**, *109*, 171.
6. Yang, S. Y.; Liu, C. I.; Wu, J. Y.; Kuo, J. C.; Huang, C. Y. *Macromol. Symp.* **2008**, *272*, 150.
7. Yoon, S. D.; Chough, S. H.; Park, H. R. *J. Appl. Polym. Sci.* **2007**, *106*, 2485.
8. Zhou, X. Y.; Cu, Y. F.; Jia, D. M.; Xie, D. *Polym. Plast. Technol.* **2009**, *48*, 489.
9. De Azeredo, H. M. C. *Food Res. Int.* **2009**, *42*, 1240.
10. Tang, X.; Alavi, S. *Carbohydr. Polym.* **2011**, *85*, 7.
11. Xie, F. W.; Pollet, E.; Halley, P. J.; Avérous, L. *Prog. Polym. Sci.* **2013**, *38*, 1590.
12. Majdzadeh-Ardakani, K.; Nazari, B. *Compos. Sci. Technol.* **2010**, *70*, 1557.
13. Gao, W.; Dong, H. Z.; Hou, H. X.; Zhang, H. *Carbohydr. Polym.* **2012**, *88*, 321.
14. Tang, X.; Alavi, S.; Herald, T. J. *Carbohydr. Polym.* **2008**, *74*, 552.
15. Lawton, J. W.; Fanta, G. F. *Carbohydr. Polym.* **1994**, *23*, 275.
16. Jayasekara, R.; Harding, I.; Bowater, I.; Christie, G. B. Y.; Lonergan, G. T. *Polym. Test.* **2004**, *23*, 17.
17. Park, H. R.; Chough, S. H.; Yun, Y. H.; Yoon, S. D. *J. Polym. Environ.* **2005**, *13*, 375.
18. Westhoff, R. P.; Kwolek, W. F.; Otey, F. H. *Starch-Stärke* **1979**, *31*, 163.
19. Tudorachi, N.; Cascaval, C. N.; Rusu, M.; Pruteanu, M. *Polym. Test.* **2000**, *19*, 785.
20. Zou, G. X.; Jin, P. Q.; Xin, L. Z. *J. Elastom. Plast.* **2008**, *40*, 303.
21. Courgneau, C.; Domenek, S.; Guinault, A.; Avérous, L.; Ducruet, V. *J. Polym. Environ.* **2011**, *19*, 362.
22. Zygoura, P. D.; Paleologos, E. K.; Kontominas, M. G. *Food Chem.* **2011**, *128*, 106.
23. Coltelli, M. B.; Maggiore, I. D.; Bertoldo, M.; Signori, F.; Bronco, S.; Ciardelli, F. *J. Appl. Polym. Sci.* **2008**, *110*, 1250.
24. Yu, J.; Wang, N.; Ma, X. *Biomacromolecules* **2008**, *9*, 1050.
25. Corrêa, M. C. S.; Branciforti, M. C.; Pollet, E.; Agnelli, J. A. M.; Nascente, P. A. P.; Avérous, L. *J. Polym. Environ.* **2012**, *20*, 283.
26. Wang, L.; Zhu, W.; Wang, X.; Chen, X.; Chen, G. Q.; Xu, K. *J. Appl. Polym. Sci.* **2008**, *107*, 166.
27. Sudhamani, S. R.; Prasad, M. S.; Sankar, K. U. *Food Hydrocoll.* **2003**, *17*, 245.
28. McGlashan, S. A.; Halley, P. J. *Polym. Int.* **2003**, *52*, 1767.
29. Zeppa, C.; Gouanvé, F.; Espuche, E. *J. Appl. Polym. Sci.* **2009**, *112*, 2044.
30. Gao, Y. L.; Dai, Y. Y.; Zhang, H.; Diao, E. J.; Hou, H. X.; Dong, H. Z. *Appl. Clay Sci.* **2014**, *99*, 201.
31. Park, H. M.; Li, X.; Jin, C. Z.; Park, C. Y.; Cho, W. J.; Ha, C. S. *Macromol. Mater. Eng.* **2002**, *287*, 553.
32. Chang, P. R.; Wu, D. L.; Anderson, D. P.; Ma, X. F. *Carbohydr. Polym.* **2012**, *89*, 687.
33. Sreekumar, P. A.; Al-Harhi, M. A.; De, S. K. *Polym. Eng. Sci.* **2012**, *52*, 2167.
34. Lai, H. M.; Padua, G. W.; Wei, L. S. *Cereal Chem.* **1997**, *74*, 83.
35. Shi, K.; Yu, H.; Lakshmana Rao, S.; Lee, T. C. *J. Agric. Food Chem.* **2012**, *60*, 5988.
36. Ali, S. S.; Tang, X.; Alavi, S.; Faubion, J. *J. Agric. Food Chem.* **2011**, *59*, 12384.
37. Thunwall, M.; Kuthanová, V.; Boldizar, A.; Rigdahl, M. *Carbohydr. Polym.* **2008**, *71*, 583.
38. Orts, W. J.; Nobes, G. A. R.; Glenn, G. M.; Gray, G. M.; Imam, S.; Chiou, B.-S. *Polym. Adv. Technol.* **2007**, *18*, 629.

39. Qiao, X.; Jiang, W.; Sun, K. *Starch-Stärke* **2005**, *57*, 581.
40. Xu, Y.; Zhou, J.; Hanna, M. A. *Cereal Chem.* **2005**, *82*, 105.
41. Perez, C. J.; Vázquez, A.; Alvarez, V. A. *J. Therm. Anal. Calorim.* **2008**, *91*, 749.
42. Maiti, P.; Okamoto, M. *Macromol. Mater. Eng.* **2003**, *288*, 440.
43. Ma, X.; Yu, J.; Wang, N. *J. Polym. Sci. Polym. Phys.* **2006**, *44*, 94.
44. Pawlak, A.; Mucha, M. *Thermochim. Acta* **2003**, *396*, 153.
45. Huang, M. F.; Yu, J. G.; Ma, X. F. *Polymer* **2004**, *45*, 7017.
46. Majdzadeh-Ardakani, K.; Navarchian, A. H.; Sadeghi, F. *Carbohydr. Polym.* **2010**, *79*, 547.
47. Wang, N.; Zhang, X.; Han, N.; Bai, S. *Carbohydr. Polym.* **2009**, *76*, 68.
48. Ma, X. F.; Yu, J. G.; Wan, J. J. *Carbohydr. Polym.* **2006**, *64*, 267.